Macromolecules

ARTICLE

pubs.acs.org/Macromolecules

Site-Dependent Segmental Dynamics Revealed Using Broadband Dielectric Spectroscopy on Well-Defined Functionalized Polystyrenes

Sandra Plaza-García,[†,‡] Reidar Lund,[*,†,‡] Angel Alegría,[‡,§] Juan Colmenero,[†,‡,§] Jonathan Janoski,[⊥] and Roderic P. Quirk[⊥]

[†]Donostia International Physics Center, Paseo Manuel de Lardizabal 4, 20018 San Sebastián, Spain

[‡]Centro de Física de Materiales (CSIC-UPV/EHU), Materials Physics Center (MPC), Paseo Manuel de Lardizabal 5, 20018 San Sebastián, Spain

[§]Departamento de Física de Materiales, Universidad del País Vasco (UPV/EHU), Apartado 1072, 20080 San Sebastián, Spain

[⊥]Institute of Polymer Science and Polymer Engineering, The University of Akron, Akron, Ohio 44325-3909, United States

ABSTRACT:

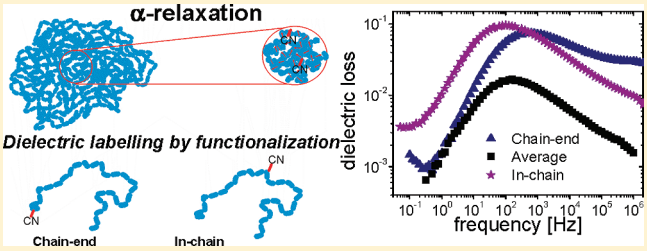

The site-dependent segmental dynamics of polystyrene has been investigated by using a combination of broadband dielectric spectroscopy (BDS) and well-defined, functionalized polystyrenes ($M_n \approx 2200$ and 4200 g/mol) with strongly polar cyano (CN) groups precisely located either at the end of the chain (chain-end functionalization) or in the middle of the chain (in-chain functionalization). Since broadband dielectric spectroscopy (BDS) is sensitive to the local dipole moment fluctuations, it is possible to selectively probe the polymer motions responsible for the dipole moment fluctuations using these cyano-functionalized polymers. By means of rheology and differential scanning calorimetry (DSC), it was confirmed that neither chain-end nor in-chain CN-functionalization affected the overall polymer matrix properties as compared with an equivalent H-functionalization analogue. This was confirmed for important properties such as the glass transition temperature (T_g) and viscosity (η). Results obtained for the two different molecular weights show that the dielectric signal associated with the chain-end fluctuations exhibits an accelerated and more heterogeneous dynamics than the average segmental α-relaxation mainly at high temperature. Closer to the T_g, the time scale of the chain-end fluctuations and the overall dynamics approach each other, and the apparent decoupling disappears. In contrast, for the segments located in the middle of the chain, the dynamics display rather similar features as the mean response although it is distinctly slower approaching T_g. This has been interpreted as combination of the intrinsic dynamic segmental heterogeneity of the polymer chain combined with the increasing cooperativity length close to T_g. The functionalization with the CN groups also allows the observation of a rather weak low-temperature relaxation process that is interpreted as a specific, more localized movement of the functional groups. The activation energies obtained are typical for motions of single molecules or segments. Interestingly, the time scale associated with this relaxation seems to decrease with molecular weight, suggesting poorer local packing for larger chains. Furthermore, the time scale depends also on the functionalization site, indicating the relevance of intermolecular interactions.

INTRODUCTION

Despite the fact that polymer dynamics has been a subject of intense investigations for many years, significant challenges to the scientific community still remain. This is basically because of the complexity of the problem: dynamics of such systems include motions on a wide range of length and time scales; from local motions such as elemental motions of individual groups, the cooperative α-relaxation of chain segments, to large-scale motions such as reptation and diffusion processes.[1]

Broadband dielectric spectroscopy (BDS) is a powerful methodology for characterizing chain dynamics of polymeric materials over broad time scales (about 10^2-10^{-9} s).[2] So far this technique has given valuable information concerning local and segmental dynamics over a very wide range of temperatures/frequencies.[2] However, BDS exhibits the limitation of being sensitive to any and all significant dipole moments present, and thus, in general, it is not a selective technique. Selectivity can be rather easily achieved in the case of multicomponent systems provided that

Received: June 27, 2011
Revised: August 25, 2011
Published: September 14, 2011

only one of the components is dielectrically active. Examples include miscible polymer blends[3,4] or block copolymer melts.[5,6] In the case of simple homopolymer melts, however, selectivity is more difficult to achieve and requires well-defined, specific functionalization. This can potentially provide a deeper understanding of specific contributions to the segmental dynamics.[7−10] Attempts to elucidate specific contributions to the segmental dynamics have been made by other techniques such as electron spin resonance spectroscopy (ESR) with spin-labeling by stable radical groups,[6,8−10] photolabeling combined with fluorescence spectroscopy,[7] photolabeling with laser spectroscopy,[11] and deuterium labeling with nuclear magnetic resonance spectroscopy (NMR) techniques.[12] In general, these studies have indicated that the chain-end mobility is higher than average showing that chain connectivity gives rise to an intrinsic heterogeneity of the segmental dynamics in polymers.[13,14] However, it is still not clear to what extent this heterogeneity deals with only a few segments at the chain-end and to what degree this effect affects the more central part of the chain. Furthermore, previously used techniques usually resolve high-frequency dynamics and can thus only be used to detect spectral changes at high temperatures well above T_g. To investigate this issue, one would need to resolve the site-dependent contributions to the overall dynamics over a wide range of temperature/frequency.

An elegant way to study specific contributions to the segmental dynamics (α-relaxation) is to utilize functionalized polymers, i.e., regular polymers with specific chemical groups attached in the backbone at precise locations, together with broadband dielectric spectroscopy (BDS). By incorporating polar functional groups that have a strong dipole moment at specific locations, relaxation processes caused by fluctuations of these molecular dipoles can be detected. In this way the different contributions to the overall chain dynamics can be separated out and distinguished. In previous studies of functionalized polymers with BDS, this has not been fully exploited for the segmental dynamics. Although end-functionalized polymers have been studied by BDS,[15−17] the technique has not been used to address specific contributions to the segmental dynamics of homopolymers. Moreover, none of the previous studies had demonstrated that functionalization does not affect the overall dynamics. Previously, the dielectric relaxation behavior of a series of well-defined (mono)functionalized polystyrenes containing only one functional group located at the end of the chain (*chain-end functionalized polymers*) was studied.[18,19] In fact, in this study, it was shown that some chain-end functional groups can significantly alter the dynamic properties[18,19] The results obtained showed that cyano (−CN) groups are ideal as selective probes since the overall polymer dynamics and matrix properties are not affected by the cyano group, in contrast to larger or interacting functional groups. Thus, in combination with BDS this is a powerful methodology to study specific dynamics and contributions to the cooperative dynamics by controlling the precise location of the functional group by well-controlled chemistry.[20,22] The advantage of polystyrene for BDS studies is the low intrinsic dielectric signal of the styrene repeat unit. Hence, the dielectric strength contribution from the segments around the functionalized group or the fluctuations of the group itself will be visible and in this way be clearly discernible from the main chain response.

In this work we have investigated the polystyrene dynamics of *chain-end* and *in-chain* cyano- and H-functionalized polystyrenes, i.e., when one cyano or H-functional group was added at the end or in the middle of the chain, respectively. Two different molecular weights were investigated: $M_n \approx 2200$ and 4200 g/mol, hereafter referred to as 2k and 4k, respectively. Precise polymer functionalization chemistry was combined with BDS as well as the complementary techniques of rheology and differential scanning calorimetry (DSC). The emphasis has been put on the segmental α-relaxation although more local relaxations have also been studied.

EXPERIMENTAL SECTION

Anionic Synthesis of In-Chain and Chain-End Functionalized Polystyrenes. All preparations of poly(styryl)lithiums (PSLi)s were effected in benzene at 303 K using *sec*-butyllithium as initiator in all-glass, sealed reactors with break-seals and standard high-vacuum techniques as described previously.[20,21] Preparations of ω-silyl hydride-functionalized polystyrenes were effected directly in the PSLi polymerization reactors by smashing break-seals for the corresponding ampules containing purified chlorodimethylsilane (1.3-fold excess) in benzene at room temperature, followed by precipitation into methanol and drying.[20] Preparations of in-chain, silyl hydride-functionalized polystyrenes were effected directly in the PSLi polymerization reactors by smashing break-seals for the corresponding ampules containing purified dichloromethylsilane ([PSLi]/[CH_3Cl_2SiH] = 2.1), in benzene at room temperature.[21] After 1 day, the unreacted PSLi was reacted with excess ethylene oxide; after 1 h, the polymer was isolated by precipitation into methanol, filtered, and dried. The in-chain, silyl hydride-functionalized polymer was isolated by silica gel column chromatography as described previously.[21]

ω-Cyano-functionalized polystyrenes were prepared by addition of 2 equiv of allyl cyanide (Aldrich, 98%) and 0.10 mL of Karstedt's catalyst (1,3-divinyltetramethyldisiloxane−platinum; Gelest, 1.2−1.4 wt % Pt in xylene) to a benzene solution of ω-silyl hydride-functionalized polystyrene in the dry box as described previously.[21] In-chain, cyano-functionalized polystyrenes were prepared by addition of 2.4 equiv of allyl cyanide and 0.10 mL of Karstedt's catalyst to a toluene solution of in-chain, silyl hydride-functionalized polystyrene in the dry box as described previously.[21] The functionalization was effected at 363 K for several days and monitored by thin layer chromatography. Additional catalyst and allyl cyanide were added as needed to drive the reaction to completion. The reference ω-propyl- and in-chain propyl-functionalized polystyrenes were prepared by pressurizing a Büchi MiniClave reactor containing either the ω-silyl hydride- or the in-chain silyl hydride-functionalized polystyrene, toluene, and Karstedt's catalyst with 100 psi of propylene (Advanced Gas Technologies, 99.5%) at room temperature for 5 days. The reaction was monitored by following the disappearance of the silyl hydride group by either FTIR (2111 cm^{-1}) or ^1H NMR (δ 3.5−4.1 ppm). The platinum catalyst residues were removed from the functionalized polymers by addition of silica gel to the product solution, stirring overnight, and then isolation by silica gel column chromatography.

Polymer Characterization. Size exclusion chromatographic analyses (SEC) for the synthesized polymers were performed using a Waters 150-C Plus instrument equipped with three HR-Styragel columns [100 Å, mixed bed (50/500/10^3/10^4 Å), mixed bed (10^3,10^4,10^6 Å)] and a triple detector system. The three detectors comprised a differential refractometer (Waters 410), a differential viscometer (Viscotek 100), and a laser light scattering detector (Wyatt Technology DAWN EOS, λ = 670 nm). THF was used as eluent with a flow rate of 1.0 mL/min at 303 K.

^1H and ^{13}C NMR spectra were acquired in $CDCl_3$ (Aldrich, 99.8% D) as solvent using a Varian Mercury 300 or Varian 500 NMR spectrometer. Infrared spectra were recorded on an Excalibur Series FT-IR spectrometer (DIGILAB, Randolph, MA) by casting polymer films on KBr plates from polymer solutions.

Differential Scanning Calorimetry (DSC). The calorimetric measurements were carried out using a Q2000 TMDSC from TA Instruments. The sample mass for these measurements was of the order of

8−10 mg. Samples were encapsulated in standard hermetic aluminum pans and a gas flow (He) was used for thermalization. Corrections for asymmetry relative to reference pan, difference in aluminum pan weight, etc., were performed using the standard procedure of online correction for the DSC Q2000 ("TzeroTM method"). The heating curves were performed using a sinusoidal temperature modulation of ±0.5 K/min every 60 s superimposed on a constant 3 K/min ramp.

Broadband Dielectric Spectroscopy (BDS). The complex dielectric permittivity, ε^*, was measured in the frequency range between 10^{-2} and 10^7 Hz using a Novocontrol high-resolution dielectric analyzer (Alpha-S analyzer). The polystyrene-based samples are brittle solids at room temperature and were prepared directly on two gold-plated electrodes with diameters of 20 and 30 mm, respectively. The samples were left to dry above T_g for an extended period of time in order to remove any residual solvent. The low molecular weight samples were dried at 403 K, whereas the higher molecular weight samples were dried at 413 K, for more than 24 h. Subsequently, while hot, the samples were squeezed between the plates using a finely cut 0.1 mm thick, star-shaped Teflon piece as spacer. These samples were kept under vacuum to remove any trapped bubbles. The data were collected isothermally in the temperature range 110−413 K, and the temperature was controlled within ±0.1 K using a Novocontrol Quatro cryostat.

Rheology. An ARES (Advanced Rheological Expansion System, TA Instruments) instrument was used for rheological measurements. Parallel plate geometry with 25 mm spacing was employed to determine the Newtonian viscosity. The sample was subjected to dynamic oscillatory shear in a range of frequencies from 0.1 to 200 rad/s. Before applying a frequency sweep, a strain sweep was performed to determine the range of linear viscoelastic response. The strain amplitude was subsequently fixed at typically 2%−10%.

RESULTS AND DISCUSSION

Polymer Synthesis. *sec*-Butyllithium-initiated, living anionic polymerization of styrene is an excellent method for preparation of polystyrenes with controlled molecular weights, narrow molecular weight distributions, and active organolithium chain-ends that can react with electrophilic linking and functionalization reagents.[22] Recently, this synthesis methodology has been combined with hydrosilyation chemistry to develop a general functionalization method for the synthesis of precisely defined, chain-end and in-chain functionalized polymers as shown in Scheme 1.[20,21] The well-defined, ω-silyl hydride (**A**)- and in-chain silyl hydride (**D**)-functionalized polystyrene intermediates can react with a variety of substituted alkenes (**B**) in the presence of a hydrosilylation catalyst (e.g., Karstedt's catalyst)[23,24] to form chain-end (**C**) or in-chain (**E**) functionalized polymers, respectively, with a variety of end groups (−**X**) as described in previous papers.[18−21] The value of this methodology for elucidation of the site-dependent segmental dynamics of polystyrene by broadband dielectric spectroscopic (BDS) studies as described herein is that a given silyl hydride-functionalized polystyrene, **A** or **D**, can be used to incorporate different functional groups, −**X**, such that the only structural variable between the two compounds is the nature of the end group, **X**. Two sets of such compounds, chain-end (**C**, **X** = **H**, **CN**) and in-chain (**E**, **X** = **H**, **CN**), have been prepared with two different molecular weights ($M_n \approx$ 2200 and 4200 g/mol), as described in Table 1. Because of the absence of structural variation other than end group, e.g. in the chain-end functionalized polymers, **C**, it was hypothesized that the polymers with only an −H "functional group" could be used as reference or model polymers to evaluate the specific contributions

Scheme 1. Methodology for the Synthesis of Polymers (P) Functionalized (a) at the Chain-End and (b) at the Middle of the Chain (In-Chain)

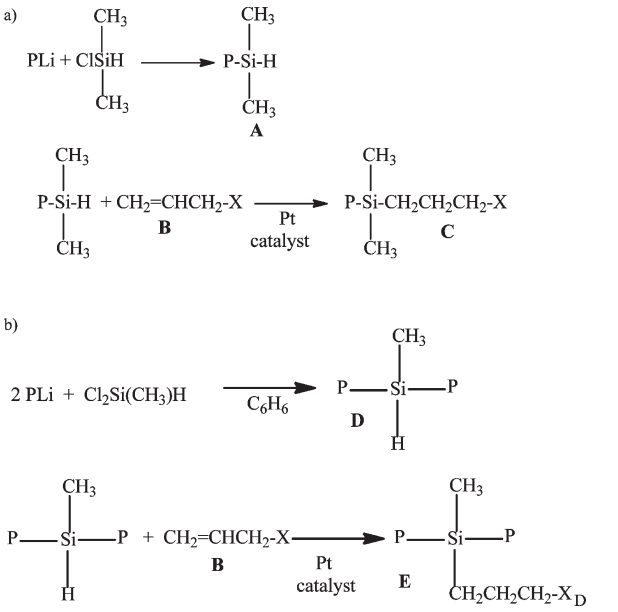

Table 1. Molecular Weights, Polydispersity Indexes, and Glass Transition Temperatures as Well as Parameters Obtained from the WLF Fits of the Viscosity Data of the Investigated Polymers

polymer	M_n [g/mol]	M_w/M_n	T_g [K]	C_1 [K]	C_2 [K]
PS-H 2k	2200	1.05	334	14.3	64.2
PS-CN 2k	2200	1.05	334	14.5	68.0
PS-H 4k	4200	1.04	354	12.8	53.9
PS-CN 4k	4200	1.04	354	12.8	54.0
PS-H-PS 2k	2300	1.02	329	14.5	54.1
PS-CN-PS 2k	2300	1.02	331	14.3	51.9
PS-H-PS 4k	4100	1.05	350	14.6	57.4
PS-CN-PS 4k	4100	1.05	351	13.1	50.9

of the −CN functional groups compared to the overall chain dynamics as delineated by BDS.

DSC and rheological results were used to characterize the overall properties of the material since these are not sensitive to any specific molecular group.

Differential Scanning Calorimetry (DSC). The resulting DSC thermograms (see Figure 1) display the curves expected for amorphous polymers without any sign of other features apart from the typical jump corresponding to a glass transition. As expected, the T_g increases with increasing molecular weight, which is usually attributed to the extra free volume induced by the chain-ends that decreases in quantity with increasing chain length. For PS it is usually observed that below a molar mass of 10 000−20 000 g/mol T_g increases strongly with molecular weight before stabilizing at a constant value of about 373 K for higher molecular weights.[25] In the present case the data show that for a given molecular weight functionalization with −H and −CN groups does not significantly affect thermal properties, since the T_g values are very similar for each pair (see Table 1).

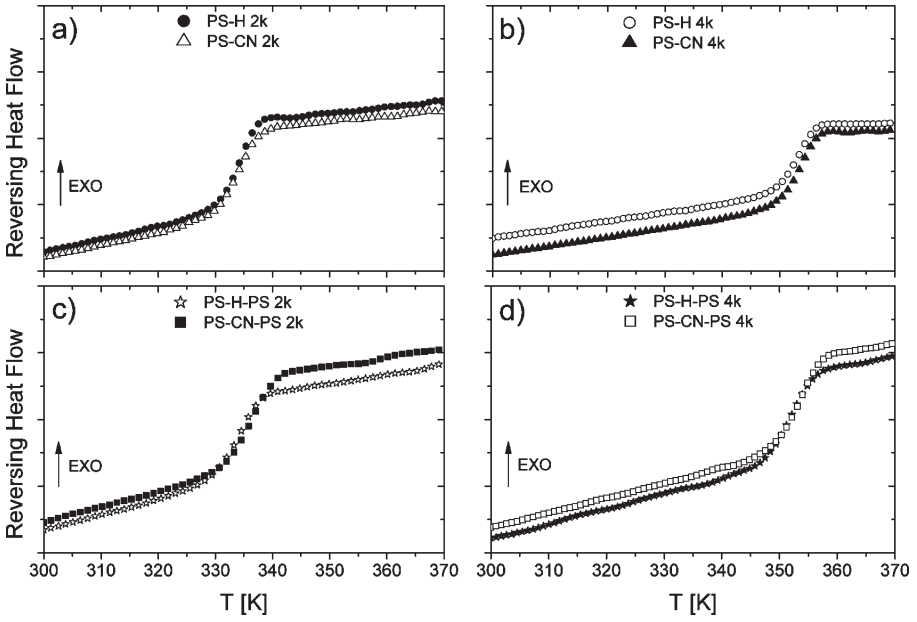

Figure 1. The reversing heat flow as a function of temperature: (a) and (b) for the chain-end 2k and 4k, respectively; and (c) and (d) for the in-chain 2k and 4k, respectively. Defining the glass transition temperatures as the inflection point of the DSC heating trace, the corresponding calorimetric T_g values are summarized in Table 1.

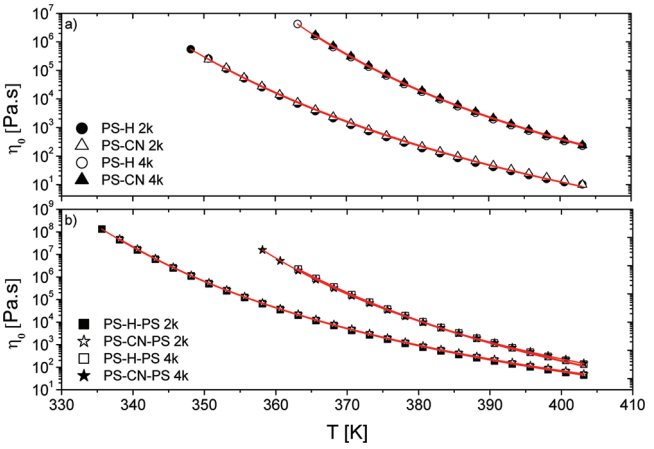

Figure 2. Zero shear viscosity, η_0, of the functionalized polymers as a function of temperature: (a) for chain-end; (b) for in-chain.

Moreover, conventional PS and the functionalized PS exhibit similar T_g values; thus, literature values for conventional PS of 2k and 4k correspond to about 323 and 345 K, respectively.[25] Therefore, when the functional group is small and noninteracting, its presence does not significantly affect the overall dynamics as probed by DSC.

Now comparing the chain-end and the in-chain functionalized polymers, it seems that placing the functional group either at the chain-end or in the middle of the chain has a minor effect on T_g. Here, only a small difference can be observed where T_g for the in-chain functionalized polymers is slightly lower than for the chain-end functionalized ones ($\cong$ 330 K vs 334 K, respectively) despite the fact that the molecular weight is slightly larger for the former. This subtle change may reflect a small added flexibility introduced by the −C−Si−C group located in the middle of the chain for the in-chain functionalized polymers (see structure **E**). In any case, these effects are not important in the context of this work. Rather, it is important to stress that the −H- and −CN-functionalized polymer pairs are essentially identical from the point of view of the calorimetric measurements.

Rheology. To extend the study of the overall dynamics to higher temperatures ($T > T_g$), rheological measurements were performed. From these experiments the zero shear viscosity, η_0, was determined at low frequencies where the viscosity appears to assume a constant "Newtonian" value.

As seen in Figure 2, the viscosities of the H-functionalized and CN-functionalized polystyrenes nearly coincide for a given molecular weight and functionalization site. The viscosity increases as the temperature decreases in a way that can be well-described using the empirical William−Landel−Ferry (WLF) equation:

$$\log \eta = \log \eta(T_g) + \frac{-\frac{C_1}{2.3}(T - T_g)}{C_2 + T - T_g} \quad (1)$$

The obtained parameters (C_1 and C_2), which are included in Table 1, again confirm that functionalization does not significantly affect polymer properties since they are comparable with the WLF parameters (corresponding to a conventional PS) taken from the literature,[1] which are C_1 = 13.7 and C_2 = 50.0 K.

These experimental results clearly show that CN-functionalization does not affect the overall dynamics as compared with the H-functionalization since both the rheological properties and glass transition temperatures are identical for each pair of CN-/H-functionalized polymers. This might not be surprising considering the small size and low concentration of the functional groups and is consistent with earlier results[18,19] where it was found that T_g was only affected for certain interacting or bulkier functional groups such as hydroxyl (−OH), acetate (−$OCOCH_3$, −Ac), and ethyl ether (−OCH_2CH_3, −OEt).

In essence, the observed invariance of both the rheological and calorimetric properties upon monofunctionalization shows that

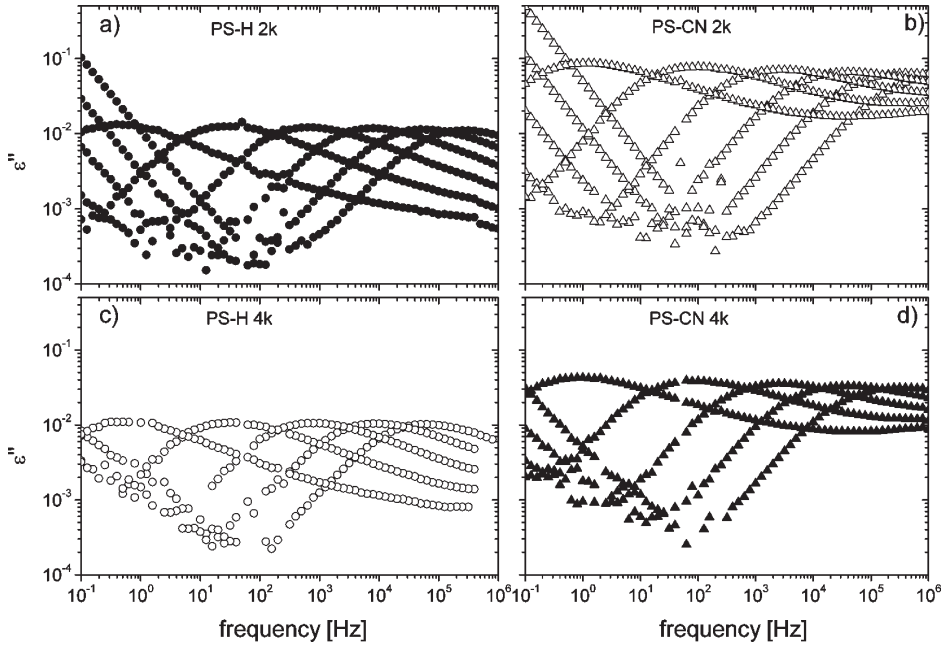

Figure 3. Dielectric segmental relaxation spectra showing the loss permittivity as a function of frequency for the chain-end functionalized polystyrenes at the following temperatures (10 K interval from right to left starting from: 388 to 338 K in the case of 2k and from 398 to 358 K in the case of 4k).

the H/CN polystyrene pairs are identical from an overall dynamics point of view. As will be shown in the subsequent section, this allows dielectric measurements to be used as a selective tool to evaluate the specific contributions to the segmental dynamics.

Broadband Dielectric Spectroscopy (BDS). Taking advantage of the results above showing that the overall dynamics of the functionalized PS are unaffected by changing from −H to −CN functionalization, one can now directly investigate the specific dynamics. Around the CN-functionalized segments, the dipole moment will be large and dominant compared to the styrene repeating units. The loss permittivity of the H-functionalized PS (the reference) provides a measure of the matrix contribution to the CN-functionalized PS data. The dielectric spectra showing the loss part of the complex permittivity, ε'', as a function of frequency for several temperatures are shown for all samples in Figures 3 and 4 for the chain-end and in-chain functionalized polymers, respectively.

As seen in Figures 3 and 4, irrespective of molecular mass and functionalization site all spectra of the CN-functionalized polymers display much stronger dielectric signals, i.e., almost 1 order of magnitude higher, than the corresponding reference (H-functionalized) polymers. This difference increases with decreasing molecular weight, which shows that this effect can be attributed to the dilution of polar groups when the molecular weight is doubled. In fact, by directly comparing the dielectric losses, approximately a factor of about 2 between the signals from the 2 versus the 4 kg/mol samples is observed. Thus, in the case of the PS-CN, the losses that are observed are dominated by the fluctuating chain-ends, whereas for the chain-end reference, PS-H, basically a weak background signal of all PS segments constituting the backbone is observed. In contrast, in the case of the in-chain functionalized polymers, the dielectric relaxation spectra for PS-CN-PS reflect the fluctuations at the center of the main polymer chain.

Concerning the shape of the dielectric spectra, it can be seen that the dielectric relaxation function related with the fluctuations of the chain-ends is broad and a high-frequency tail contribution is observed, which cannot be resolved as a peak at lower temperatures. This tail can be associated with the specific CN end-group fluctuations. However, this extra contribution is not present when the CN functional group is located in the middle of the chain. In this case, a dynamic behavior similar to the reference is found. This phenomenology is observed for both molecular weights.

Summarizing, the peak positions shift to higher frequency and the shape becomes broader, indicating that the dynamics is faster and more heterogeneous for the CN chain-end functionalized PS with respect to that of PS-H reference. In contrast, the CN in-chain functionalized PS presents a similar time scale and shape as compared to the PS-H-PS reference.

To quantify the differences in the temperature dependence of the dielectric relaxation, the main relaxation times data (calculated as the reciprocal of the loss peak, f_{max}, according to $\tau^* = 1/(2\pi f_{max})$) (see Figure 5) have been fitted with a Vogel−Fulcher−Tamman (VFT) equation:

$$\log \tau^* = \log \tau_0 + \frac{B}{T - T_0} \qquad (2)$$

where τ_0 is the elemental time scale, T_0 the so-called Vogel temperature, and B a factor describing the apparent activation energy in the high temperature limit. The obtained parameters are included in Table 2. Using these values, it was found that the so-called dynamic glass transition temperatures (T_{gD}), which here has been defined as the temperature at which the dielectric relaxation time takes a value of 10 s, are in good agreement with the values obtained from DSC experiments (see Table 1); the differences in all cases are less than 2 K. This is not a trivial result in particular for the CN-functionalized polymers and will be discussed in detail later in the article.

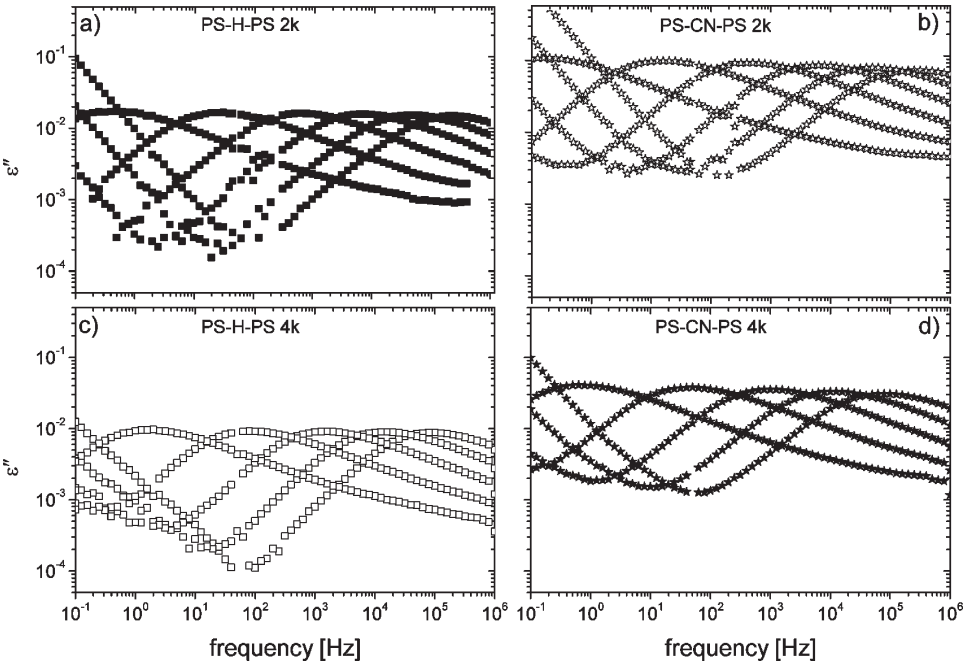

Figure 4. Dielectric relaxation spectra showing the dielectric loss permittivity as a function of frequency for the in-chain functionalized polystyrenes at the following temperatures (10 K interval from right to left starting from: from 388 to 338 K in the case of 2k and from 398 to 358 K in the case of 4k).

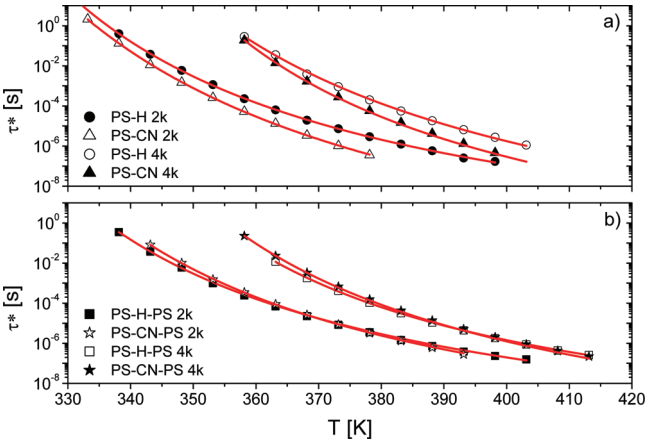

Figure 5. Temperature dependence of the main α-relaxation time of the functionalized polymers: (a) for chain-end; (b) for in-chain functionalized polymers.

The fragility index introduced by Angell[26] is defined as $|m = (\partial \log(\tau_\alpha))/\partial T|_{T=T_g}$ and can be calculated from the VFT formula in a straightforward manner which gives

$$m = \frac{1}{\ln 10}\frac{B}{T_g}\frac{1}{(1 - T_0/T_g)^2} \quad (3)$$

As seen in Table 2, the values of m in the case of the H-functionalized polymers are essentially the same (85−89), independent of molecular weight and functionalization (in-chain/chain-end). These are typical values for an intermediately "strong" glass and similar to the values for conventional PS at these low molecular weights.[27] Generally, the fragility index of PS is found to increase with molecular weight; in the current limited range there is no apparent increase between 2k and 4k.

Table 2. Parameters Obtained from the Vogel−Fulcher−Tamman Fits of the Main α-Relaxation Time of the Functionalized Polymers[a]

polymer	τ_0 [s]	B [K]	T_0 [K]	T_{gD} [K]	m
PS-H 2k	7.1×10^{-14}	1735.8	279.0	332.3	88
PS-CN 2k	7.0×10^{-14}	1430.9	287.4	331.3	107
PS-H 4k	9.1×10^{-15}	2067.7	291.6	351.3	89
PS-CN 4k	5.8×10^{-15}	1726.8	302.6	351.8	109
PS-H-PS 2k	2.0×10^{-13}	1640.0	280.0	332.0	87
PS-CN-PS 2k	9.7×10^{-14}	1653.4	282.9	333.9	92
PS-H-PS 4k	2.1×10^{-14}	2021.0	288.0	347.9	85
PS-CN-PS 4k	5.7×10^{-14}	1691.3	299.8	351.4	97

[a] The calculated "dielectric glass transition temperature" T_{gD} and the "fragility index", m, are also included (see text for details).

Now comparing with the chain-end functionalized polymers, it is obvious that end segment fluctuations, which give rise to a higher measured mobility observed mainly well above T_g, translate to a higher fragility index (107−109) and thus a more "fragile" character. This directly shows that the increased fragility index reported with increasing molecular weight of PS[27] cannot be easily related to chain-ends, as the fraction of the chain-ends decreases with m. Neither is it directly related to the increase in flexibility of the chain-end, since chain flexibility of polymers is expected to decrease the fragility index. In the present case, the difference is that different dynamics belonging to the same polymer having the same overall T_g is probed. Obviously, the chain-end dynamics displays a higher fragility index that is directly related to the already mentioned decoupling of the chain-end from the overall dynamics as the temperature increases.

Local Secondary Relaxation Dynamics. At temperatures well below the glass transition, secondary relaxations are usually observed by BDS and are attributed to local dipole moment

dx.doi.org/10.1021/ma2014436 |*Macromolecules* 2011, 44, 7810–7819

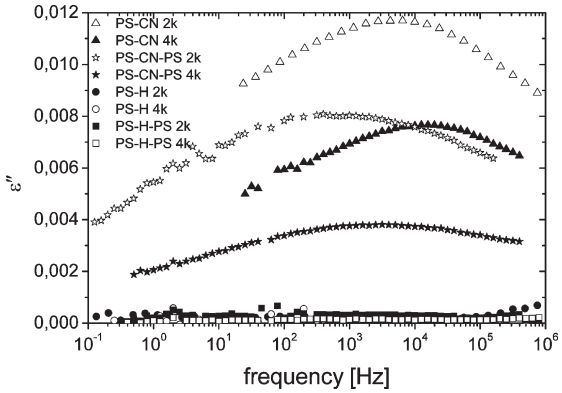

Figure 6. Dielectric relaxation at low temperatures showing the frequency dependence of the dielectric loss permittivity at a temperature of 120 K for the chain-end and in-chain functionalized polymers.

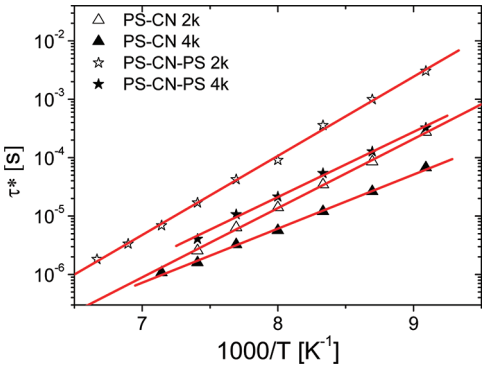

Figure 7. Temperature dependence of the secondary dielectric relaxation time for CN-chain-end and in-chain functionalized polystyrenes. Lines are fits to the Arrhenius equation. See text for details.

fluctuations. As has been reported earlier,[18,19] the CN-functionalized polystyrenes present a clear peak in the dielectric loss spectrum at temperatures much lower than T_g. This secondary dielectric relaxation process could be related to local conformational rearrangements. The corresponding loss peaks are depicted in detail in Figure 6 for all the samples at 120 K. As expected, the H-functionalized polymers do not show any significant signal. However, in the case of the cyano-functionalized polymers a clear dielectric response can be observed. These results show the rather localized movement of the CN group as the origin of such process.

As was shown for the segmental dynamics, the secondary relaxation process of the CN-functionalized polymers has a higher intensity for the lower molecular weights due to the dilution effect already mentioned. Now concerning the shape and peak frequency of the dielectric spectra, it is observed that, whereas shape is not much affected, dynamics become faster for higher molecular weights. Also, functionalization site plays an important role in the dynamics since the chain-end functionalization leads to a response that is faster than the in-chain functionalization.

From the loss peak frequency, the main relaxation times, τ^*, have been obtained, which are shown in Figure 7.

As expected for a localized motion, this temperature dependence can be well fitted using the well-known Arrhenius equation:

$$\tau = \tau_0^s \exp\left(\frac{E_A}{k_B T}\right) \quad (4)$$

where E_A is the activation energy, τ_0^s is a prefactor related to an attempt frequency, and k_B is the Boltzmann constant.

The activation energy values obtained for the CN-functionalized polymers are reported in Table 3. It is interesting to see that, as it was already seen for the peak positions of the dielectric spectra, there is a slight but significant difference in the values of the activation energy for the two molecular weights. Here E_A is always smaller for the high molecular weight. This can most likely be attributed to a difference in the local packing around the functional group. This fact, in addition to the observed difference between the chain-end and in-chain functionalized polymers, suggests that the activation energy is not only controlled by rotational barriers within the whole functional group: $Si-CH_2-CH_2-CH_2-CN$.

Table 3. Parameters Describing the Arrhenius Temperature Dependence of the Secondary Dielectric Relaxation Processes for the CN-Functionalized Polystyrenes

polymer	E_A[kJ/mol]	τ_0^s [s]
PS-CN 2k	24.5	9.20×10^{-16}
PS-CN 4k	19.8	3.57×10^{-14}
PS-CN-PS 2k	25.9	1.13×10^{-15}
PS-CN-PS 4k	21.3	2.39×10^{-14}

Specific Contributions to the Segmental Dynamics. The main objective of this work was to investigate the specific contributions of the different parts of the chain to the segmental relaxation. The approach followed here consisted of extracting the "pure" chain-end and in-chain fluctuation dynamics from the overall dynamics by subtracting the response of the reference (H-functionalized) polymer from that of the corresponding CN-functionalized polymer. This methodology was applied for both chain-end and in-chain as well as for the two different molecular weights. In Figure 8 the results of this approach are shown for representative temperatures (353 and 373 K for the 2k and 4k samples, respectively) that correspond to about 20 K above the respective glass transition temperatures.

This approach is based on the idea that the dielectric response coming from the corresponding reference sample (H-functionalized) reflects the contribution to the overall dynamics of the polymer chain in the absence of a significant dipole moment of the H-functional group. However, this is not the case for the CN-functionalized polymer where the fluctuation of the functional group makes the dielectric response much higher. Hence, as seen directly from Figure 8a,b, most of the signal in the case of PS-CN comes from the CN group fluctuating at the end of the chain. As already mentioned, this contribution not only displays a general accelerated dynamics compared to the mean chain (average) response but also becomes much more heterogeneous with a prominent tail toward high frequencies whose contribution cannot be resolved as a peak even at lower temperatures. On the contrary, when the CN group is situated in the middle of the chain as for the in-chain functionalized polymers depicted in Figure 8c,d, even though again the CN groups contribute to most of the signal, the shapes of the spectra are very similar to the reference response.

dx.doi.org/10.1021/ma2014436 |*Macromolecules* 2011, 44, 7810–7819

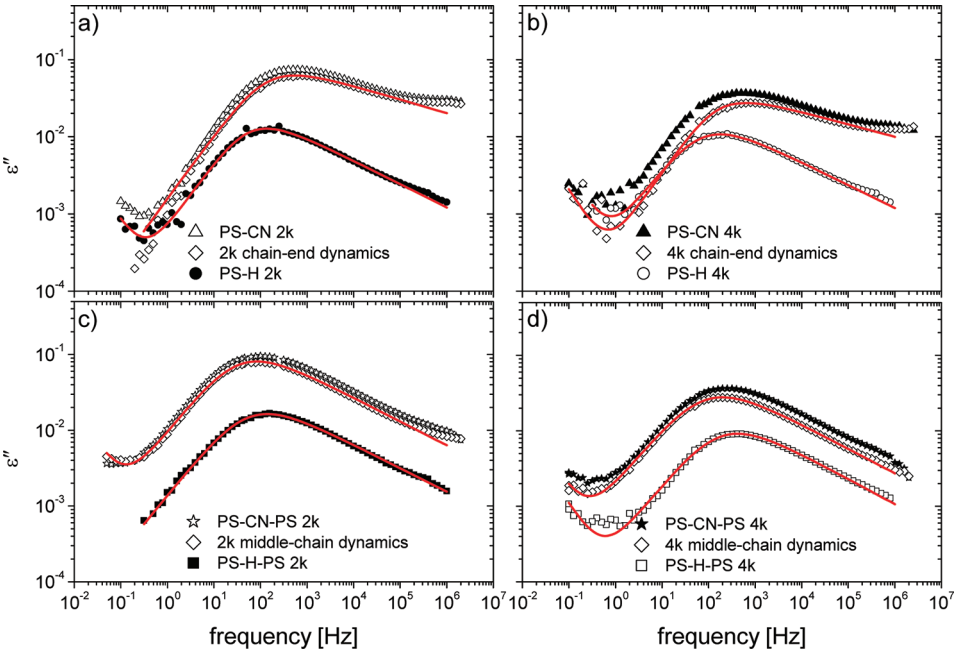

Figure 8. Comparison of the dielectric spectra of the CN-functionalized polystyrenes and the corresponding references. To facilitate comparisons, the results are displayed at temperatures that correspond to about 20 K above T_g. The chosen temperatures are 353 and 373 K for the 2k and 4k, respectively. The lines display fits using the parametrization given in the main text using eq 5.

Table 4. Fit Parameters and Related Quantities Extracted from an Analysis of the Dielectric Loss Spectra Shown in Figure 8 Using a Havriliak−Negami Parameterization

polymer	$\Delta\varepsilon$	α	γ	fwhm[28] (decades)
PS-H 2k	0.054	0.85	0.35	2.70
end-chain 2k	0.372	0.83	0.21	4.12
PS-H 4k	0.047	0.80	0.37	2.81
end-chain 4k	0.171	0.88	0.18	4.39
PS-H-PS 2k	0.072	0.77	0.40	2.78
middle-chain 2k	0.353	0.77	0.40	2.74
PS-H-PS 4k	0.039	0.76	0.44	2.66
middle-chain 4k	0.123	0.74	0.44	2.74

In order to extract more quantitative information concerning the shape of the dielectric spectra, these data were analyzed in terms of an empirical Havriliak−Negami expression:

$$\varepsilon''(\omega)_{HN} = \mathrm{Im}\left[\frac{\Delta\varepsilon}{(1 + (i\omega\tau_{HN})^{\alpha})^{\gamma}}\right] \quad (5)$$

where $\Delta\varepsilon$ is the dielectric relaxation strength and τ_{HN} is a characteristic time, whereas α and γ ($0 < \alpha \leq 1$ and $0 < \gamma \leq 1$) are parameters describing symmetric and asymmetric broadening of the dielectric spectrum, respectively.

In order to compare the response coming from the in-chain, chain-end, and the overall dynamics, the 2k data at 353 K and the 4k data at 373 K in Figure 8 were analyzed using eq 5 in addition to a conductivity term [$\varepsilon_{cond} \propto 1/\omega$] visible at low frequencies of the loss spectra. The results are displayed in Figure 8, and the resulting parameters are given in Table 4.

As observed in Figure 8, all of the data for the in-chain CN-functionalized and the H-reference polymers can be described

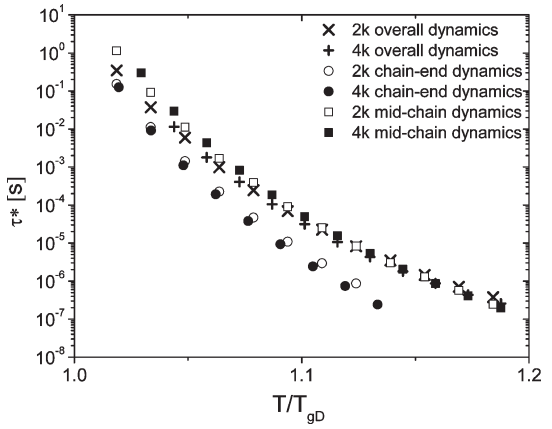

Figure 9. Scaled temperature dependence of the characteristic relaxation time (τ^*) for overall dynamics as compared with the time scale of the chain-end segments fluctuations and middle-chain segments fluctuations.

rather perfectly with the Havriliak−Negami function over the whole frequency range. From the fits, very similar parameters are deduced with α parameters of about 0.76−0.8 and γ of about 0.4. This is reflected in very similar fwhm values calculated from the HN-function. For the chain-end fluctuations, however, it is clearly seen that a simple HN-function is not enough to describe the data at high frequency. As previously mentioned, this asymmetric broadening is a signature of another contribution that cannot be resolved wholly as a peak but is related to the chain-end fluctuations. This high-frequency tail-like contribution is also reflected in very low values for γ of about 0.2 (see Table 4).

In Figure 9, the site-dependent segmental relaxation times are compared in a temperature scaled representation, which removes the trivial variations originated from minor T_g changes. All the

dx.doi.org/10.1021/ma2014436 |*Macromolecules* 2011, 44, 7810–7819

data has been normalized to the T_{gD} of the corresponding reference H-functionalized polymer.

As seen in Figure 9, for the chain-end dynamics there is a clear separation of the time scale at high temperatures, which can be understood in terms of considerably faster than average motions of the end segments. However, as the temperature is getting lower and closer to T_g, both time scales start approaching each other. On the contrary, for the middle chain segments the relaxation times appear to be almost the same at high temperatures whereas at lower temperatures (about $T/T_{gD} < 1.1$) the time characteristic of the center of the chain fluctuations becomes slightly larger than the average. Higher chain-end mobility compared to mid-chain segments was already reported in works by Miwa and co-workers[8−10] in the high-temperature limit. However, the present results further show that this difference in mobility tends to disappear when approaching the glass transition from above. This has been possible thanks to the extremely broad frequency range available by dielectric spectroscopy compared to other techniques.

The previous findings can be tentatively understood as originating from a sort of gradient of segmental mobility along the polymer chain. With such a view, the results show that at high temperatures the chain-ends move substantially faster than average, whereas the motion at the center of the chain is very similar to the latter. This would explain also why the dielectric signal corresponding to the chain-end fluctuations extends significantly more toward higher frequencies, since it is partially decoupled from the overall dynamics. This feature is not related with specific dynamics of the functional group itself since it is not detected for in-chain functionalization. Therefore, it is indicative of an intrinsic dynamic aspect of the polymer chain-ends. In considering segments away from the end groups, at high temperatures the dynamics would be rather homogeneous since the center of the chain fluctuations behaves similarly to the average. On the other hand, at lower temperatures we see that the chain-end and average segmental relaxation times approach. This can be a signature of the growing cooperativity[28] that would involve a collective motion of many segments together with those of the chain-ends. This would make the chain-end relaxation time slower than average as T_g is approached from above (higher fragility index). This would be because at lower temperatures the dynamics reflects a cooperative movement of many types of segments rather than the specific part where the CN group is located. In contrast, for the in-chain functionalization, we see that at low temperatures the center part of the chain displays a dynamics slightly slower than the average. This may be interpreted as an effect of the local surrounding of the center-part of the chain, which contains less chain-end segments than the average, as a consequence of chain connectivity. Thus, the contribution to the whole segmental-relaxation from this part is slower than the average.

In addition, when considering the shape of the dielectric response from the CN in-chain functional group, one observes that the spectra are very similar to that of the average dynamics. There is also a much less pronounced high-frequency contribution compared to the chain-end functionalized polymers which indicates a more homogeneous behavior.

CONCLUSIONS

This work has shown how a sophisticated synthesis methodology can be used to label polymer chains by selectively introducing functional groups at the chain-end or in the middle of the chain and how this in combination with BDS, DSC, and rheology has allowed us to extract detailed aspects of the polymer segmental dynamics.

The above experimental results clearly show that functionalization of polystyrene with −H and −CN groups does not modify significantly the properties expected for a conventional polystyrene. Moreover, by taking the H-functionalized PS as the reference, it has been observed that changing the functional group by a −CN group the overall matrix properties remain practically unaltered since both the rheological properties (viscosity) and T_g are nearly identical for each pair of H/CN-functionalized polymers. This fact has been confirmed for two different molecular weights and functionalization sites. By BDS we have been able to analyze the site-dependent segmental dynamics. In this way, it can be concluded that the chain-end polystyrene segments exhibit a faster as well as more heterogeneous dynamics, the former being more pronounced at higher temperatures. On the contrary, the dynamics of the middle of the chain polystyrene segments is similar to the average, although it gets slightly slower close to T_g. Therefore, on one hand, these results indicate noticeable contributions to heterogeneity from the chain-end segments, and on the other hand, the rest of the segments along the polymer chain present a rather similar dynamical behavior.

AUTHOR INFORMATION

Corresponding Author
*E-mail: reidar_lund@ehu.es.

ACKNOWLEDGMENT

The Government of the Basque Country (GIC07/35-IT-463-07) and the Spanish Ministry of Education (MAT 2007-63681/CSD2006-00053) are gratefully acknowledged for support.

REFERENCES

(1) Ferry, J. D. *Viscoelastic Properties of Polymers*, 3rd ed.; John Wiley & Sons: New York, 1980.
(2) Kremer, F., Schönhals, A., Eds. *Broadband Dielectric Spectroscopy*; Springer-Verlag: Berlin, 2003.
(3) Miwa, Y.; Sugino, Y.; Yamamoto, K.; Tanabe, T.; Sakaguchi, M.; Sakai, M.; Shimada, S. *Macromolecules* **2004**, *37*, 6061.
(4) Colmenero, J.; Arbe, A. *Soft Matter* **2007**, *3*, 1474.
(5) Lund, R.; Willner, L.; Alegría, A.; Colmenero, J.; Richter, D. *Macromolecules* **2008**, *41*, 511.
(6) Miwa, Y.; Yamamoto, K.; Sakaguchi, M.; Sakai, M.; Tanida, K.; Hara, S.; Okamoto, S.; Shimada, S. *Macromolecules* **2004**, *37*, 831.
(7) Horinaka, J.; Maruta, M.; Ito, S.; Yamamoto, M. *Macromolecules* **2003**, *32*, 1134.
(8) Miwa, Y.; Tanase, T.; Yamamoto, K.; O.; Sakaguchi, M.; Sakai, M.; Shimada, S. *Macromolecules* **2003**, *36*, 3235.
(9) Miwa, Y. *Macromolecules* **2009**, *42*, 6141.
(10) Miwa, Y.; Shimada, S.; Urakawa, O.; Nobukawa, S. *Macromolecules* **2010**, *43*, 7192.
(11) Sung, C. S. P.; Gould, I. R.; Turro, N. J. *Macromolecules* **1984**, *17*, 1447.
(12) Metin, B.; Blum, F. D. *Polym. Prepr.* **2006**, *47* (1), 43.
(13) Fox, T. G.; Flory, P. J. *J. Appl. Phys.* **1950**, *21*, 581.
(14) Fox, T. G.; Flory, P. J. *J. Polym. Sci.* **1954**, *14*, 315.
(15) Mijovich, J.; Sun, M.; Han, Y. *Macromolecules* **2002**, *35*, 6417.
(16) Floudas, G.; Fytas, G.; Pispas, S.; Hadijichristidis, N.; Pakula, T.; Khoklov, A. R. *Macromolecules* **1995**, *28*, 5109.
(17) Soccio, M.; Nogales, A.; García-Gutierrez, M. C.; Lotti, N.; Munari, A.; Ezquerra, T. A. *Macromolecules* **2008**, *41*, 2651.

(18) Lund, R.; Plaza-García, S.; Alegría, A.; Colmenero, J.; Janoski, J.; Chowdhury, S. R.; Quirk, R. P. *Macromolecules* **2009**, *42*, 8875.
(19) Lund, R.; Plaza-García, S.; Alegría, A.; Colmenero, J.; Janoski, J.; Chowdhury, S. R.; Quirk, R. P. *J. Non-Cryst. Solids* **2010**, *356*, 676.
(20) Quirk, R. P.; Kim, H.; Polce, M. J.; Wesdemiotis, C. *Macromolecules* **2005**, *38*, 7895.
(21) Quirk, R. P.; Janoski, J.; Chowdhury, S. R.; Wesdemiotis, C.; Dabney, D. E. *Macromolecules* **2009**, *42*, 494.
(22) Hsieh, H. L.; Quirk, R. P. *Anionic Polymerization: Principles and Practical Applications*; Marcel-Dekker: New York, 1996.
(23) Marciniec, B. *Comprehensive Handbook on Hydrosilylation*; Pergamon Press: Oxford, 1992.
(24) Brook, M. A. *Silicon in Organic, Organometallic, and Polymer Chemistry*; John Wiley & Sons: New York, 2000.
(25) Ding, Y.; Kisliuk, A.; Sokolov, A. P. *Macromolecules* **2004**, *37*, 161.
(26) Angell, C. A. *J. Non-Cryst. Solids* **1985**, *73*, 1.
(27) Sokolov, A. P.; Novikov, V. N.; Ding, Y. *J. Phys.: Condens. Matter* **2007**, *19*, 205116.
(28) Adam, G.; Gibbs, J. H. *J. Chem. Phys.* **1965**, *43*, 139.